OPEN

IGF1 and CXCR4 Respectively Related With Inhibited M1 Macrophage Polarization in Keloids

Ying Liu, MD,*† Bing Han, MD,† Liuchang Tan, MD,‡ Dongshuo Ji, MD,* and Xiaofang Chen, MD§

Purpose: The pathophysiology of keloid remains unclear. Exploring the immune heterogeneity and new biomarkers of keloids can help design new therapeutic targets for keloid treatments and prevention.

Methods: The authors performed single-cell RNA sequencing analysis and bulk data differential gene expression analysis of public datasets(GSE92566 and GSE163973). They used Gene Ontology (GO), Gene Set Enrichment Analysis (GSEA), and immune infiltration analysis to identify the function of the differential expressed genes. Besides, the authors performed qt-PCR on keloid tissue and adjacent normal tissues from 3 patients for further verification.

Results: M2 macrophage increased in keloid samples than M1 macrophage. The authors identified 2 potential novel biomarkers of keloid, IGF1 and CXCR4, which could inhibit M1 macrophage polarization. The potential mechanism could be inhibiting immune responses and anti-inflammatory activities through INF signaling and E2F targeting. The differential expression of the 2 genes was verified by clinical samples.

Conclusions: The authors identified 2 immune signaling molecules associated with keloid formation (IGF1 and CXCR4) and analyzed their potential pathogenic mechanisms.

From the *Department of Plastic Surgery, Beijing Hospital of Integrated Traditional Chinese and Western Medicine; †Department of Scar & Wound Treatment, Plastic Surgery Hospital, Chinese Academy of Medical Sciences and Peking Union Medical College; §Department of Plastic and Reconstructive Surgery, Beijing Chaoyang Hospital, Capital Medical University, Beijing; and ‡Department of Plastic and Cosmetic Surgery, Daping Hospital, Army Medical University, Chongqing, China.

Address correspondence and reprint requests to Dongshuo Ji, MD, Department of Plastic Surgery, Beijing Hospital of Integrated Traditional Chinese and Western Medicine, Beijing 100038, China; E-mail: jidongshuo@126.com; Xiaofang Chen, MD, Department of Plastic and Reconstructive Surgery, Beijing Chaoyang Hospital, Capital Medical University, Beijing 100016, China; E-mail: xiaofang_chen2020@163.com
Y.L., B.H., and L.T. contributed equally to this work.

Keloids are fibrous, proliferative, prominent skin scar–like lesions of the skin, characterized by a persistent, gradual growth beyond the wound margins into the surrounding healthy skin.[1] Due to the characteristics of keloids, they can cause severe pain, chronic pruritus, psychosocial impairment, and motor striction to the patients, which leaves a heavy burden.[2,3]

Since keloids are mainly characterized by increased proliferation of fibroblasts and extensive overproduction of exocellular matrix (ECM) components, research on keloids has primarily focused on the role of fibroblasts in keloid development. Although these studies have shined light on some potentially pathogenic factors, the fundamental driving pathos-mechanistic events remain unclear.[1] Recently, several researchers have noticed that the surrounding immune microenvironment can play a vital role in the development of keloids. The increased number of T cells, Langerhans cells, mast cells, and macrophages in keloid compared to normal tissues is associated with skin fibrosis.[4,5] The keloid fibroblasts and immune cells can interact with each other and develop synergically and complex regulation of molecules and pathways, which contribute to the development of keloids. Among these immune cells, macrophages play a key role in cutaneous wound healing by modulating the microenvironment during the different healing phases.[6–8] In particular, M2 macrophages are associated with fibrosis and scarring and persist in keloids.[4,9] Martin Direder[10] found that macrophages in keloids predominantly display an M2 polarization, and their crosstalk with Schwann cell contributes to the continuous expansion of keloids. Chao[11] found more macrophages were activated toward the M2 subtype in the keloid dermis when compared with the normal dermis, and fibroblast in keloid has a higher phosphorylated STAT6 (p-STAT6) level, which is a known inducer of M2 polarization when compared with fibroblasts in the normal dermis. Thus, keloid formation might be associated with M2 macrophage polarization, but little is known about the cause of this phenomenon.

Single-cell sequencing analysis is a revolutionary research method[12] that allows the clustering of the cells to study the

differences in gene expression among different groups and the differences in cell development trajectory.[13] In this study, we delved into the immune cell population in keloids and found that an abnormal reaction of M2-type macrophage to skin injuries contributes to keloid pathogenesis.

METHODS

Data Acquisition

We downloaded 1 keloid RNA microarray data set (GSE92566) and 1 keloid single-cell RNA sequencing data set (GSE163973) from the GEO database for differential gene expression analysis. After normalization, samples without grouping information were excluded, resulting in 6 samples in GSE92566 and 6 paired tissue samples in GSE163973. Immune-related genes were obtained from ImmPort[14] (Supplemental Digital Content 1, Table 1, http://links.lww.com/SCS/G510). Four RNA microarray data sets (GSE44270, GSE145725, GSE7890, and GSE92566) are downloaded for immune filtration analysis. A brief introduction of these data sets and samples included are listed in Supplemental Digital Content 1, Table 1, http://links.lww.com/SCS/G510.

Single-Cell Data Processing and Clustering

Single-cell data processing and clustering are done with the "Seurat" R package (Version: 3.0.1). Cells with genes expressed between 300 and 5500, and <10% mitochondrial genes are selected. And 1053 immune cells were retained in total. Then the top 2500 highly variable genes were selected for downstream analysis, the first 20 principal components (PCs) were chosen to do cell clustering, and the UMAP plot was adopted to show the immune cell cluster. For the annotation of each cluster, we used the "Find All Markers" function in the Seurat package to find significant markers in each cluster and used the "Single R" package to annotate the cell type for every cluster.

Pseudotime Analysis

When the cell type of all clusters was annotated, we used the Monocle (version: 3.0) R package for subsequent pseudotime analysis. The dimensionality of the cells was reduced by the principal component analysis (PCA) method, and then the type of cell differentiation status was calculated by the "Reduce Dimension" function. We used the "Find All Markers" function to find genes that differed significantly across states. Finally, we use the "plot_cell_trajectory" function to display a trajectory map of cell differentiation.

Differential Gene Analysis in Array Data

The original data of GSE92566 were processed with the "affy" R package (version 1.68.0). Differential gene analyses between the keloid and normal skin were performed using the "limma" package (version 2.46.0). We set the threshold of $log2|$ fold change$| > 1$ and $P < 0.05$ to obtain the differentially expressed genes (DEGs). The DEGs were visualized with heatmap and volcano map by the "pheatmap" package (version 1.0.12) and the "ggplot2" package (version 3.3.3).

Protein-Protein Interaction (PPI)

The STRING database (version 11.0)[15] was used to construct the protein-protein interaction (PPI) network. Moreover, we used the MCODE plug-in (version 1.32)[16] in Cytoscape (version 3.8.2)[17] to identify densely connected networks.

Identification of DEIGs

We took the intersection of the differential genes between keloid samples and normal scar samples obtained by single-cell analysis, the differential genes obtained by GSE92566, and the immune-related genes obtained from ImmPort finally got 6 immune-related DEGs (DEIGs).

Gene Enrichment Analysis

The "clusterProfiler" package (version 3.18.1)[18] was used for gene set enrichment analysis (GSEA),[19] disease ontology,[20] and gene ontology[21] enrichment analysis to understand the biological processes involved in the DEGs from each step.

Immune Infiltration Analysis

We conducted an immune infiltration landscape analysis based on CIBERSORT[22] to estimate the abundance of immune cell types in keloid and normal samples using DEG expression data in the array data.

Clinical Validation

Each of the 3 Keloid samples and adjacent normal skin samples are collected during the surgical procedure. These samples are paired. This study was approved by the ethics committee of Peking Union Medical College & Plastic Surgical Hospital (Beijing, China), and the patients provided signed written informed consent before enrollment.

Statistical Analysis

All the statistical analyses were carried out based on R software. Comparisons of single gene expression between keloid and normal groups were performed using the Student t test. The Student t test was performed to compare the clinical variables. Unless otherwise specified, $P < 0.05$ is considered significant.

RESULTS

Single-Cell Data Processing and Clustering

We processed the single-cell RNA-seq data of GSE163973 and the quality control of the data (Fig. 1A), we set the threshold as nFeature_RNA > 1000 and nFeature_RNA < 6000 and percent.mt < 15 for filtering the cells. After quality control, we took the 1053 immune cells from the data set for downstream analysis and picked out the top 2500 highly variable genes for downstream analysis (Fig. 1B). After dimension reduction, these cells are divided into 9 clusters (Fig. 1C) and are roughly annotated as monocytes, dendritic cells, and macrophages. We used macrophage markers to re-annotate the 2 macrophage subclusters (Fig. 2A), and we found that although most markers both expressed in the 2 clusters, M1 macrophage markers like CCR5, IL6, MARCO, and PPARG are highly expressed in cluster 3 (Fig. 2A), and M2 macrophage markers like CD36, CD209, FCGR3A, MERTK, SIGLEC1, and TLR4 are highly expressed in cluster 2, so we re-named the 2 macrophage clusters as M1 macrophage and M2 macrophage.

Enrichment Analysis Showed Lymphocytes Activation and Immune Response Different Between Keloid and Normal Scar

Next, we compared differences between keloid immune cells and normal scar immune cells. Compared with a normal scar, we set the threshold as p values < 0.05, avg_logFc > 0.5, and Difference (which represents the difference value of the percentage of cells expressing each gene) > 0.1,[23] and finally, there are 109 genes upregulated and 85 genes downregulated in the keloid immune cells (Fig. 2B). Gene ontology (GO) analysis
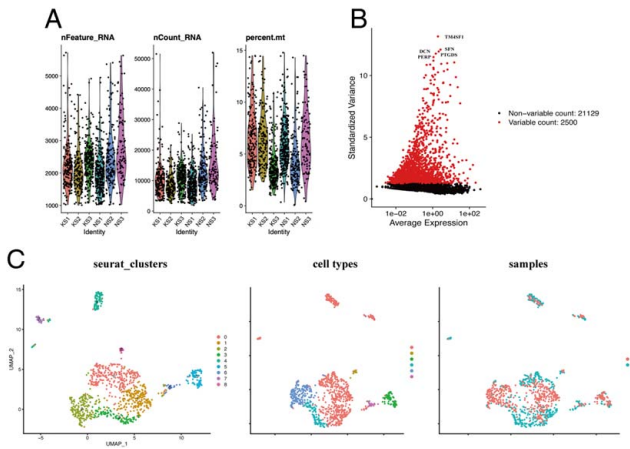
FIGURE 1. Single-cell RNA-seq reveals the immune landscape in keloid and normal scar tissue. (A) Quality control of the single-cell RNA-seq data in GSE163973. (B) Three thousand highly variable genes labeled in red are selected for downstream dimension reduction. The top 10 genes are highlighted with gene names. (C) Unbiased clustering of 1053 cells reveals 9 cellular clusters. The clustering of immune cells is annotated as 6 immune cell types. Clusters or cell types are distinguished by different colors. The general identity of each cell cluster is shown on the right. All clusters and cell types are shown in both samples. DC I indicates dendritic cell group I; DC II, dendritic cell group II; KS, keloid samples; NS, normal scar.

suggested that pathways about immune response, response to bacterial infection, and wound healing are activated in the normal scar (Fig. 2C), while leukocyte and lymphocyte activation and proliferation-associated pathways were enriched in keloid immune cells (Fig. 2D).

Macrophages Distribute Different Properties in Keloid and Normal Scar

Based on the clues from the enrichments result of the differential expressed genes (DE genes) above, we next compared the proportions of the cell populations and cell cycle between keloid and normal scare. After removing the cell cycle bias ef-

FIGURE 2. Enrichment analysis showed lymphocyte activation and immune response difference between keloid and normal scar. (A) Heatmap showing macrophage markers expressing among Seurat subclusters. Highly different expressed M1 and M2 macrophage markers are labeled. (B) Volcano plot shows the percentage difference (Different Percent of Cells) and log-fold change based on the Wilcoxon rank-sum test results for differential gene expression comparing between keloid normal scar. Genes in red are genes highly expressed in keloid, and genes in blue are genes highly expressed in the normal scar. (C) GO analysis with enriched GO terms for various pathways for genes highly expressed in normal skin and (D) for genes highly expressed in keloid.

fect, we still found differences among different cell types. All cell types consist of 3 cell circle phases with the G1 phase dominant, except for the monocytes, which are absent of G1 phase cells (Fig. 3A, B). The macrophage cells presented the most variance in cell cycle phase variance between keloids and normal scars (Fig. 3B). Meanwhile, the immune cells of keloids and normal scars showed distinct relative cell number ratios, the macrophage subpopulations also distributed the most variance (Fig. 3C). Increased proportions were observed for M1 type macrophage in the normal scar and M2 type macrophage in the keloid. The M2 proportion increased in the keloid and decreased in the normal scar tissue, which is consistent with previous reports.[4,9]

Next, we explored the differentially expressed genes between M1 and M2 clusters and found 28 genes highly expressed while 33 genes down expressed in the M2 macrophage compared with the M1 macrophage (Fig. 3D). The GSEA enrichment analysis showed 2 pathways enriched in the DE genes (Fig. 3E). The Hall marker MYC targets V2 pathway was activated (Fig. 3F), while the IL6/JAK/STAT3 signaling was suppressed in the keloid (Fig. 3G).

Differential Gene Analysis in Bulk Data

We performed differential expression analysis on the chip data set GSE92566, which contains 3 keloid samples and 3 paired normal skin samples. A total of 1526 genes are obtained with the threshold of log2FC >1 and *P* value <0.05. Among them, 850 genes are downregulated, while 676 genes are upregulated in the keloid samples compared with paired adjacent normal skin (Fig. 4A, B). We intersected them with the 2483 immune-related genes we obtained from the ImmPort database, and we got 120 immune-related DG genes (IRDGs). We performed enrichment analysis with these IRDGs to infer their functions, and the GO enrichment results and GSEA enrichment results all suggested mesenchyme-related pathways, like mesenchyme development, epithelial-mesenchymal transition, and mesenchymal cell differentiation (Fig. 4C, D). These results suggest the immune cells in the keloid could stimulate mesenchymal cell proliferation and transition. Both the results showed that IL6, JAK, and STAT3 signaling could play a vital role in the development of the keloids. And also, interestingly we found that neuron-related pathways like axon extension and neuron projection extension are involved in the GO enrichment results (Fig. 4C).

Expression Profile of the Key Genes in Keloid and Normal Tissue

We intersect the 194 differential genes of single-cell macrophages and the 120 immune-related differential genes in data set GSE92566, as shown in the Venn graph (Fig. 5A); finally, we obtain 6 key genes, which are DCD, CXCR4, CMTM3, IGF1, AQP9, and PTGER2 (Supplemental Digital Content 2, Table 2, http://links.lww.com/SCS/G511). Genes of DCD, CXCR4, CMTM3, and IGF1 are highly expressed in the keloid immune cells compared with normal scar immune cells in the single-cell data, while the other 2 are low expressed (Fig. 5D, E, Supplemental Digital Content 3, Figure 1, http://links.lww.com/SCS/G512). In the keloid samples in the array data, genes of CXCR4, CMTM3, and IGF1 are highly expressed compared with the adjacent normal skin tissue, while the other 3 genes are low expressed (Fig. 5B, C). We also noticed that, in the single-cell data, IGF1 was exclusively expressed in cluster 2, which is the M2 macrophage, and CXCR4 was widely expressed in all clusters except for cluster 4, which is a small group of dendritic cells.
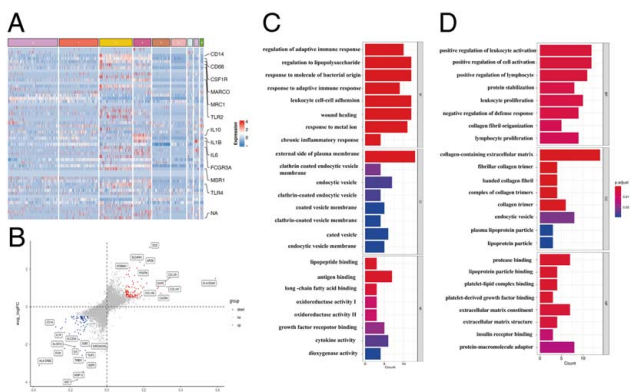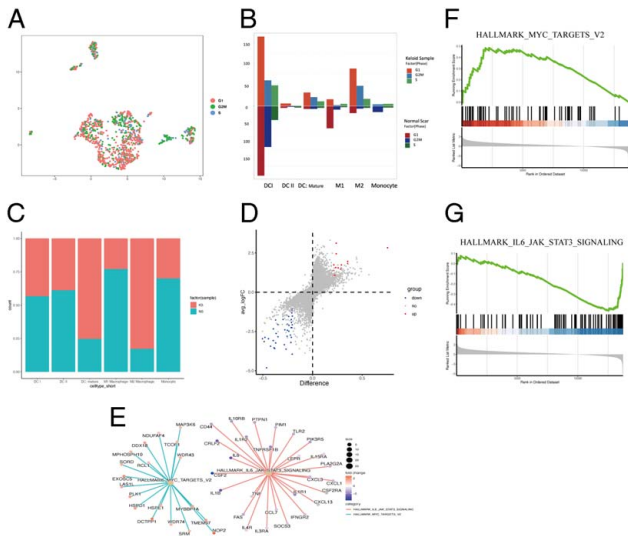
FIGURE 3. Macrophages distribute different properties in keloid and normal scar. (A) UMAP plot of all the immune cell clusters based on cell cycle features. Cells are colored with respect to their cell cycle phase. (B) Bar plot shows different cell phase counts in each cell type. Up: in the keloid sample, down: in the normal scar sample. (C) Bar plot shows the different percentages of each cell type in keloid samples and normal scar samples. (D) Volcano plot shows the percentage difference (Different Percent of Cells) and log-fold change based on the Wilcoxon rank-sum test results for differential gene expression comparing genes in red are genes highly expressed in keloid and genes in blue are genes highly expressed in the normal scar. (E) Dot plots for GSEA enrichment plots for representative signaling pathways enriched in M2 macrophage compared with M1 macrophage. Genes highly expressed in M2 macrophages are in red colors and genes low expressed in M2 macrophages are in blue colors. (F) GSEA pathway MYC-target-V2 activated. (G) GSEA pathway IL6-JAK-STAT3 suppressed. KS indicates keloid samples; NS, normal scar.
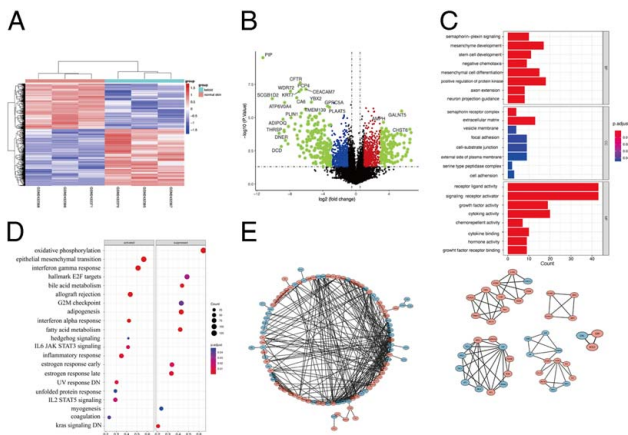

FIGURE 4. Differential gene analysis in GSE92566. (A) Heatmaps show the differential gene analysis results between keloid and adjacent normal skin. Gene expression levels are correlated with the red and blue color. (B) Volcanic maps of differential genes. Blue dots represent genes that are low-expressed in keloid tissue, compared with adjacent normal skin, and red dots represent genes that are high-expressed. Genes with logFC > 3 or logFC < -3 are labeled in green colors. (C) GO analysis with enriched GO terms for various pathways for genes differentially expressed. (D) GSEA analysis results for genes differentially expressed. (E) Protein-protein interaction (PPI) network for 120 immune-related DE genes, each dot represents 1 gene and is colored by expression. The red dot means upregulated genes, while the blue color means downregulated genes. MCODE results showed 5 key gene modules.
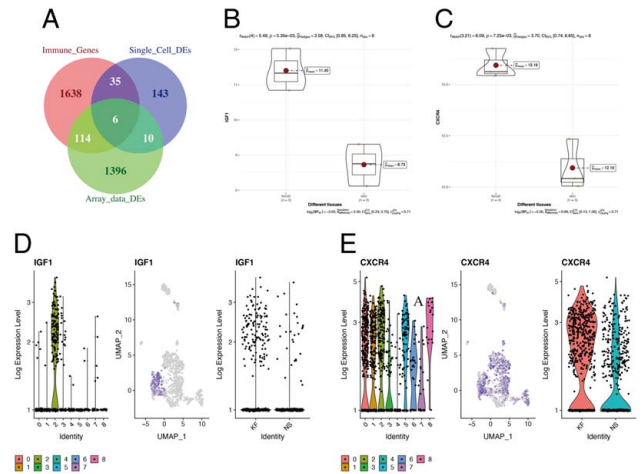

FIGURE 5. Expression levels of key genes in single-cell data and array data. (A) The Venn plot shows the intersection of differentially expressed genes in single-cell data and in array data and the immune-related genes. (B, C) IGF1 and CXCR4 expression analysis in array data set GSE92566. IGF1 and CXCR4 expression are upregulated in keloid. (D, E) IGF1 and CXCR4 expression in the single-cell data. The gene expression is presented between Seurat clusters (left), in the UMAP feature plot (middle), and between different samples (right).

Functions of Key Genes in Macrophage Development

To further explore the functions of these key genes on macrophage differentiation and polarization, we first analyze the correlation between these gene expression levels of immune infiltration. We selected 26 samples of keloid tissues from 4 RNA microarray data sets (GSE44270, GSE145725, GSE7890, and GSE92566) to perform immune infiltration analysis (Supplemental Digital Content 1, Table 1, http://links.lww.com/SCS/G510). T cells, including memory-resting CD4 T cells and CD8 T cells, are dominant in the infiltrated immune cells (Fig. 6A, B). For the macrophage lineage, all the M0, M1, and M2 phenotypes are presented in the keloid samples, and M2 showed the highest proportion, while M0 and M1 macrophage proportions are relatively low.

Then, according to the expression levels of each key gene, we divided the 26 samples into the high-expression group and the low-expression group. We found that M1 macrophage both increased in the low-expression group of CXCR4 genes and IGF1 genes (Fig. 6C, D), and the M1 macrophage proportion was negatively related with the expression level of CXCR4 and IGF1 respectively (Supplemental Digital Content 4, Figure 2, http://links.lww.com/SCS/G513), which indicates that the high expression of these 2 genes would inhibit M1 macrophage polarization.

Cell Differentiation Trajectory of All the Immune Cells

In order to find out when and how these genes initiated their suppress function, we first simulated the cell differentiation trajectory of all the immune cells and plotted the expression of CXCR4 and IGF1 along the pseudotime (Fig. 7A, B). Considering the macrophage lineage development process and the cell cycle results, we selected monocytes as the starting node, and the results showed that the macrophage groups are in a middle pseudotime phase. The expression of CXCR4 started at the beginning of this trajectory, then decreased, and increased again with the appearance of the macrophage groups, and then
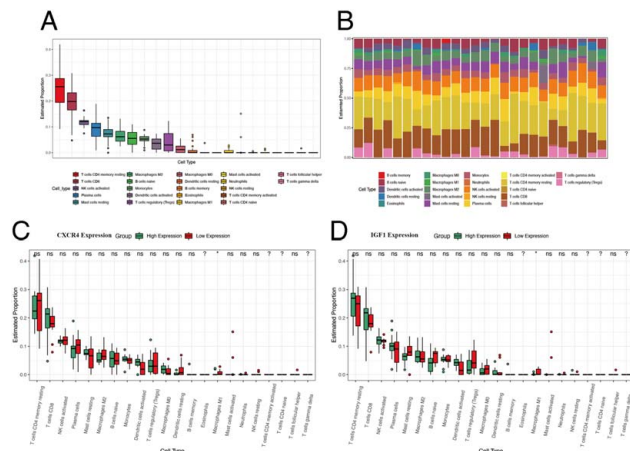
FIGURE 6. Immune infiltration analysis in array data. (A) Box plot showed the immune landscape of keloids. Different cell types are presented with different colors. (B) Immune cell type proportion in each sample. Each column represents each keloid sample, and different cell types are presented with different colors, as labeled below. (C) The immune cell infiltration proportion between the CXCR4 high-expression level group and the CXCR4 low-expression level group. The green color represents the high-expression group, and the red color represents the low-expression group. (D) The immune cell infiltration proportion between the CXCR4 high-expression level group and the IGF1 low-expression level group. *P* values are labeled above each column. *$P < 0.05$, **$P < 0.01$, ***$P < 0.001$. ns: not significant. ?: means certain cell types are not infiltrated in the samples.

decreased at the end of the trajectory (Fig. 7B). And the expression of IGF1 was only exhibited at the macrophage phase (Fig. 7B). These results indicate that these 2 genes may be related to macrophage development during the pathogenic process in the keloid.

Then, we performed GSEA analysis in the high-expression and low-expression groups of CXCR4 and IGF1 separately in the 26 keloids array data. The result showed that in the high-expression group of both CXCR4 and IGF1, pathways of IFN-γ response, IFN-α response, and E2F targets are all sup-
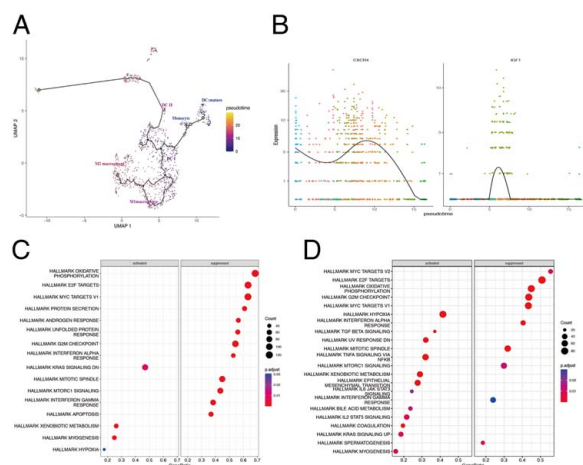

FIGURE 7. Function analysis for IGF1 and CXCR4. (A) Pseudotime analysis for immunes in the single-cell data. Darker blue indicates earlier differentiation, and light yellow indicates late differentiation. (B) CXCR4 and IGF1 expression arranged in the trajectory of pseudotime differentiation. The dark line represents gene expression level, and the dots represent cells queued according to the pseudotime. The cells are colored with Seurat clusters. (C) GSEA enrichment analysis results in differentially expressed genes according to CXCR4 expression groups and (D) IGF1 expression groups.

pressed while pathways of myogenesis and hypoxia are activated (Fig. 7C, D).

Clinical Validation for IGF1 and CXCR4

We use qPCR to test the expression of IGF1 and CXCR4 in keloid samples and normal skin for clinical validation, in quantities of 3 for each sample. The results (Fig. 8) show that both IGF1 and CXCR4 were significantly highly expressed in keloids compared with normal skin.

DISCUSSION

Although keloid disease has been extensively studied, key mechanisms leading to the development of keloid have still not been elucidated and understood. In addition, treatments to prevent or treat keloid are scarce and not effective.

Immune systems are known to regulate atypical fibroblast proliferation, myofibroblast transformation, and collagen I accumulation during abnormal scar formation.[24] Keloid is known to be infiltrated with macrophage, but how this macrophage regulates the process of keloid development remains unclear. Herein, we analyzed the public single-cell dataset and array dataset and explored the characteristics and key regulatory pathways of distinct immune cell types. These findings will help us understand keloid pathogenesis in-depth and provide potential targets for clinical therapies of keloids.

Evidence showed that the increased number of M2 macrophages and decreased/equal number of M1 macrophages play a vital role in scar susceptibility.[25,26] In a prospective study,[27] the authors investigated baseline M2 macrophages in the local wound-healing environment by performing biopsies immediately after the incision. During the follow-up, the group of patients who developed HTS had higher baseline M2 macrophages (CD68^{+}, CD206^{+}) compared with patients presenting with normal scars. Butzelaar et al[28] measured the macrophages of skin samples from both keloid susceptible sites (eg, earlobes, mandible, neck, and shoulders) and nonsusceptible sites (eg, the upper eyelid, cheek, and abdomen). The results showed that significantly fewer numbers of M1 macrophages (CD40^{+}) were observed at the susceptible sites of keloid formation, but equal numbers of M2 macrophages (CD163^{+}) were observed at the susceptible and nonsusceptible sites.[28]

The increased M2 macrophage and decreased/equal M1 macrophage phenomenon were also observed in our findings. The single-cell landscape showed higher M2 macrophages and fewer M1 macrophages in the keloid sample and an inverted ratio in the normal scar sample. The immune infiltration results in the 26 keloid samples also showed higher M2 infiltration and lower M1 infiltration proportion. The relation between the M2/M1 infiltration and the progress of keloid and HTS is not well elucidated. A possible explanation for the association between increased preinjury M2 macrophages and HTS formation could be that tissue-resident macrophages altered the immune microenvironment to suppress adaptive immune responses, including M1 macrophages, thereby favoring HTS and keloid formation.[29] This could be supported by our enrichment analysis results. In the GO analysis for DEGs between keloid and normal scar samples of the single data, pathways of lymphocyte activation, negative regulation of defense response, and adaptive immune response are enriched, and in the keloid groups, overexpression of IGF-1 or CXCR4, the pathway of interferon-gamma response and interferon-alpha response is suppressed. But in DEGs between keloid and adjacent normal skin, the pathway of interferon-gamma response and interferon-alpha response is activated in the keloid; we think that is because the
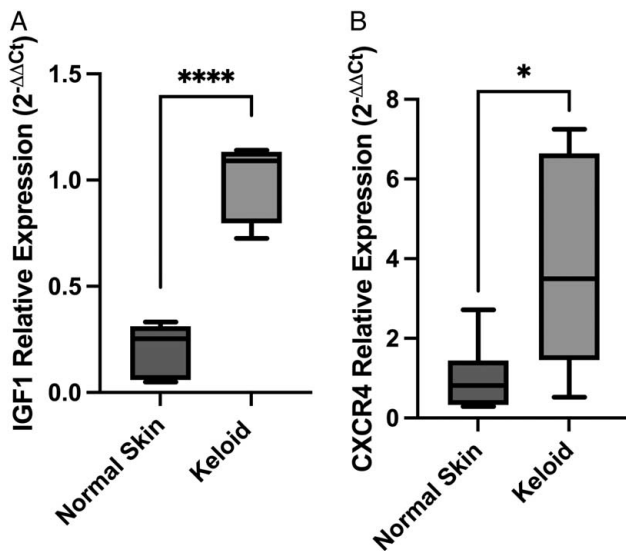
FIGURE 8. Clinical validation for IGF1 and CXCR4. (A) qPCR results for CXCR4 expression in normal skin and keloid samples (n = 3). (B) qPCR results for IGF1 expression in normal skin and keloid samples (n = 3). *P < 0.05.

keloid shows persistent neoplastic proliferation beyond the wound margin and invasion of adjacent normal skin, so the adjacent skin showed a similar micro-environment or severe immune suppression. The results of keloid and remote normal skin should show opposite results.

After differential gene analysis and functional analysis, we found two genes, IGF1 and CXCR4, that could play a role in regulating the orchestra of macrophage functions during the keloid development process. The expression of 2 genes in the keloid sample may suppress the polarizations of the M1 macrophage. Typically, IGF1 is exclusively expressed in the Seurat 2 cluster, which is the M2 macrophage. We hypothesize that the overexpression of M2 macrophage in the keloid had negative feedback for the M1 polarization, which would aggravate the disproportion of M2/M1 macrophage in the keloid formation process. This hypothesis could be supported by the enrichment results we obtained. In the GSEA result of the IGF1 and CXCR4 high-expression keloids, we found that the pathways of E2F targets, IFN-γ response, and IFN- α response are all suppressed.

The activation of M1/M2 macrophage phenotypes depends on cytokines from adaptive immune cells (such as IFN-γ from Th1 cells or IL-4 from Th2 cells).[30] Interferon-γ (IFN-γ) has been identified as a key factor for inducing tumoricidal M1 phenotype in macrophages and shown to synergize with TLR agonists for induction of macrophage tumoricidal activity and production of both NO and proinflammatory cytokines (TNF-α, IL-12p40, and IL-12p70). Besides IFN-γ which is type II INF, less toxic type I IFNs like IFN-α and IFN-β could also synergize with TLR agonists for induction of M1 macrophage tumoricidal activity and production of both NO and proinflammatory cytokines (TNF-α, IL-12p40, and IL-12p70).[31] IFN-γ and IFN-α also showed an antifibrotic effect. In an experimental renal fibrosis model, selective administration of interferon-γ results in the amelioration of fibrosis with reduced collagen synthesis and a-SMA production.[32] Lee et al[33] gave intra-local keloid lesion injections of IFN-α2b combined with tretinoin to keloid patients and reported a therapeutic improvement rate of more than 80% in most cases. Wang et al[34] reported that the number of fibroblasts in the proliferating scar of HTS patients was significantly reduced by systematic

administration of IFN-α2b and that IFN-α2b dose-dependently prevented the differentiation of peripheral blood mononuclear cells into fibroblasts as demonstrated in vitro.

The E2F family can also mediate the macrophage M1/M2 polarization and immune response. E2F transcription factors play critical roles in the cell cycle. E2F1, as a transcription factor, can activate the transcription activity of IL-6 promoter, and modulate macrophage function through a microenvironment manner. E2F1 knockout mouse model showed that M2 polarization could be enhanced through increased PPAR-γ expression in E2F1 knockout mice.[35] E2F2 directly regulates the STAT1 and NF-kB pathways to exacerbate the inflammatory phenotype in rheumatoid arthritis.[36] Retinoblastoma (RB) tumor suppressor inactivation, which activates the E2F activity, enhances proinflammatory signaling through stimulation of IL-6/STAT3 signaling.[37]

The suppressed E2F signaling and INF signaling helped to explain the over-activated M2 macrophage and inhibited M1 macrophage in the keloid samples.

The IGFs are members of a family of insulin-related peptides that include Relaxin and several peptides isolated from lower invertebrates.[38] IGF-1 is a small peptide consisting of 70 amino acids with a molecular weight of 7649 Da.[27] The structural similarity to insulin explains the ability of IGF-1 to bind to the insulin receptor. IGF-I and IGF-II have been shown to facilitate wound healing by stimulating fibroblast proliferation and enhancing collagen synthesis.[39] And evidence shows that IGF-1 plays a part in the pathogenesis of keloids and hypertrophic scar (HTS). IGF-I accounted for the invasive growth of fibroblast as well as the excessive production of ECM proteins induced by TGF-b.[40] Shih et al[41] found IGF-1 significantly increased in keloid tissue when compared with normal fibroblast. Hu et al[42] analyzed IGF-1R expression by immunohistochemistry, real-time PCR, and western blotting on tissues and fibroblasts from 30 patients and found IGF-IR is predominantly expressed on dermal fibroblasts. Daian et al[43] found that IGF-1 only had a minor effect on fibroblast proliferation; however, the invasiveness of keloid fibroblast was significantly enhanced by IGF-1 stimulation, which was shown to be done through the PI3K pathway.[44] However, these studies all focused on the fibroblast, and little was reported on IGF-1 on immune filtration, especially on macrophage function in keloids. However, whether IGF-1 could have a regulatory function in keloid macrophage cells, has not been explored. But in human T lymphocytes, IGF-1 could downregulate IFN- γR2 chain surface expression and desensitize IFN-γ/STAT-1signaling, thus inhibiting the T-cell apoptosis.[45–47] Our results showed that the same mechanisms may also work in M1 macrophage in the keloid formation process but require further bench experiment confirmation.

CXCR4/ CXCL12 axis has been found to play a role in a variety of cellular trafficking events, both in health and disease conditions and in cancer metastasis and infiltration. Chris A Campbell et al compared the CXCR4/CXCL12 expression in the circulating fibrocytes between keloid patients and normal patients and found CXCR4 expression level was significantly higher in the former.[48] Fibrocytes expressing CXCR4 are brought into circulation in response to CXCL12, and within target tissues, local mediators affect differentiation and cellular function.[49–51] Both in vitro and in vivo studies have demonstrated that inhibition of fibrocyte chemotaxis through the CXCR4/CXCL12 axis has halted collagen deposition in response to noxious stimuli.[52,53] Our results of public data analysis suggest the overexpression of CXCR4 in keloid may also have macrophage recruiting functions.

During this project, we found it hard to get homogeneous sample states across different public data sets. Typically, the keloid is a persistent process and can show different gene expression features between the formation states and mature states; moreover, the normal skin of the keloid or HTS patients may not be that "normal." The heterogeneity of public data sets is a deficiency of this study; also, the number of clinical samples in our study is limited, and more benchworks, both in vivo and in vitro, are needed in the future.

CONCLUSIONS

We identified 2 potential novel biomarkers of keloid, IGF1 and CXCR4, through single-cell analysis, array data, and differential expression analysis. These 2 genes inhibit M1 polarization in keloid pathogenesis by regulating INF signaling and E2F targets, thus inhibiting immune responses and anti-inflammatory activities. Therefore, it is tempting to speculate that the M2 polarization is a result of inhibiting M1 polarization, and this imbalance in polarization could potentially serve as a promising treatment option. Our study offers a new perspective on the pathogenesis of keloids, which has the potential to greatly enhance the treatment of this skin disease in the future.

REFERENCES

1. Limandjaja GC, Niessen FB, Scheper RJ, et al. The keloid disorder: heterogeneity, histopathology, mechanisms and models. *Front Cell Dev Biol* 2020;8:360
2. Balci DD, Inandi T, Dogramaci CA, et al. DLQI scores in patients with keloids and hypertrophic scars: a prospective case control study. *J Dtsch Dermatol Ges* 2009;7:688–692
3. Alhady SM, Sivanantharajah K. Keloids in various races. A review of 175 cases. *Plast Reconstr Surg* 1969;44:564–566
4. Bagabir R, Byers RJ, Chaudhry IH, et al. Site-specific immunophenotyping of keloid disease demonstrates immune upregulation and the presence of lymphoid aggregates. *Br J Dermatol* 2012;167:1053–1066
5. Jiao H, Fan J, Cai J, et al. Analysis of characteristics similar to autoimmune disease in keloid patients. *Aesthetic Plast Surg* 2015; 39:818–825
6. Lucas T, Waisman A, Ranjan R, et al. Differential roles of macrophages in diverse phases of skin repair. *J Immunol* 2010;184: 3964–3977
7. Mirza R, DiPietro LA, Koh TJ. Selective and specific macrophage ablation is detrimental to wound healing in mice. *Am J Pathol* 2009; 175:2454–2462
8. Zhu Z, Ding J, Ma Z, et al. Systemic depletion of macrophages in the subacute phase of wound healing reduces hypertrophic scar formation. *Wound Repair Regen* 2016;24:644–656
9. Boyce DE, Ciampolini J, Ruge F, et al. Inflammatory-cell subpopulations in keloid scars. *Br J Plast Surg* 2001;54:511–516
10. Direder M, Weiss T, Copic D, et al. Schwann cells contribute to keloid formation. *Matrix Biol* 2022;108:55–76
11. Chao H, Zheng L, Hsu P, et al. IL-13RA2 downregulation in fibroblasts promotes keloid fibrosis via JAK/STAT6 activation. *JCI Insight* 2023;8(6):e157091.
12. Nomura S. Single-cell genomics to understand disease pathogenesis. *J Hum Genet* 2021;66:75–84
13. Deng CC, Hu YF, Zhu DH, et al. Single-cell RNA-seq reveals fibroblast heterogeneity and increased mesenchymal fibroblasts in human fibrotic skin diseases. *Nat Commun* 2021;12: 3709
14. Bhattacharya S, Dunn P, Thomas CG, et al. ImmPort, toward repurposing of open access immunological assay data for translational and clinical research. *Sci Data* 2018;5:180015
15. von Mering C, Huynen M, Jaeggi D, et al. STRING: a database of predicted functional associations between proteins. *Nucleic Acids Res* 2003;31:258–261
16. Bader GD, Hogue CW. An automated method for finding molecular complexes in large protein interaction networks. *BMC Bioinform* 2003;4:2
17. Shannon P, Markiel A, Ozier O, et al. Cytoscape: a software environment for integrated models of biomolecular interaction networks. *Genome Res* 2003;13:2498–2504
18. Yu G, Wang LG, Han Y, et al. clusterProfiler: an R package for comparing biological themes among gene clusters. *OMICS* 2012;16: 284–287
19. Hanzelmann S, Castelo R, Guinney J. GSVA: gene set variation analysis for microarray and RNA-seq data. *BMC Bioinform* 2013;14:7
20. Bello SM, Shimoyama M, Mitraka E, et al. Disease ontology: improving and unifying disease annotations across species. *Dis Model Mech* 2018;11:dmm.032839.
21. Ashburner M, Ball CA, Blake JA, et al. Gene ontology: tool for the unification of biology. The Gene Ontology Consortium. *Nat Genet* 2000;25:25–29
22. Chen B, Khodadoust MS, Liu CL, et al. Profiling tumor infiltrating immune cells with CIBERSORT. *Methods Mol Biol* 2018;1711: 243–259
23. Direder M, Wielscher M, Weiss T, et al. The transcriptional profile of keloidal Schwann cells. *Exp Mol Med* 2022;54:1886–1900
24. van der Veer WM, Bloemen MC, Ulrich MM, et al. Potential cellular and molecular causes of hypertrophic scar formation. *Burns* 2009;35:15–29
25. Hesketh M, Sahin KB, West ZE, et al. Macrophage phenotypes regulate scar formation and chronic wound healing. *Int J Mol Sci* 2017;18:1545
26. Xu X, Gu S, Huang X, et al. The role of macrophages in the formation of hypertrophic scars and keloids. *Burns Trauma* 2020;8: tkaa006
27. Rinderknecht E, Humbel RE. The amino acid sequence of human insulin-like growth factor I and its structural homology with proinsulin. *J Biol Chem* 1978;253:2769–2776
28. Butzelaar L, Niessen FB, Talhout W, et al. Different properties of skin of different body sites: the root of keloid formation? *Wound Repair Regen* 2017;25:758–766
29. Rodero MP, Khosrotehrani K. Skin wound healing modulation by macrophages. *Int J Clin Exp Pathol* 2010;3:643–653
30. Mosser DM, Edwards JP. Exploring the full spectrum of macrophage activation. *Nat Rev Immunol* 2008;8:958–969
31. Muller E, Christopoulos PF, Halder S, et al. Toll-like receptor ligands and interferon-gamma synergize for induction of antitumor M1 macrophages. *Front Immunol* 2017;8:1383
32. Inagaki Y, Nemoto T, Kushida M, et al. Interferon alfa down-regulates collagen gene transcription and suppresses experimental hepatic fibrosis in mice. *Hepatology* 2003;38:890–899
33. Lee JH, Kim SE, Lee AY. Effects of interferon-alpha2b on keloid treatment with triamcinolone acetonide intralesional injection. *Int J Dermatol* 2008;47:183–186
34. Wang J, Jiao H, Stewart TL, et al. Improvement in postburn hypertrophic scar after treatment with IFN-alpha2b is associated with decreased fibrocytes. *J Interferon Cytokine Res* 2007;27: 921–930
35. Xiao H, Wu YP, Yang CC, et al. Knockout of E2F1 enhances the polarization of M2 phenotype macrophages to accelerate the wound healing process. *Kaohsiung J Med Sci* 2020;36:692–698
36. Wang S, Wang L, Wu C, et al. E2F2 directly regulates the STAT1 and PI3K/AKT/NF-kappaB pathways to exacerbate the inflammatory phenotype in rheumatoid arthritis synovial fibroblasts and mouse embryonic fibroblasts. *Arthritis Res Ther* 2018;20:225
37. Kitajima S, Takahashi C. Intersection of retinoblastoma tumor suppressor function, stem cells, metabolism, and inflammation. *Cancer Sci* 2017;108:1726–1731
38. Blundell TL, Humbel RE. Hormone families: pancreatic hormones and homologous growth factors. *Nature* 1980;287:781–787
39. Baserga R. Oncogenes and the strategy of growth factors. *Cell* 1994; 79:927–930
40. Yoshimoto H, Ishihara H, Ohtsuru A, et al. Overexpression of insulin-like growth factor-1 (IGF-I) receptor and the invasiveness of cultured keloid fibroblasts. *Am J Pathol* 1999;154:883–889

41. Shih B, Garside E, McGrouther DA, et al. Molecular dissection of abnormal wound healing processes resulting in keloid disease. *Wound Repair Regen* 2010;18:139–153
42. Hu ZC, Tang B, Guo D, et al. Expression of insulin-like growth factor-1 receptor in keloid and hypertrophic scar. *Clin Exp Dermatol* 2014;39:822–828
43. Daian T, Ohtsuru A, Rogounovitch T, et al. Insulin-like growth factor-I enhances transforming growth factor-beta-induced extracellular matrix protein production through the P38/activating transcription factor-2 signaling pathway in keloid fibroblasts. *J Invest Dermatol* 2003;120:956–962
44. Song J, Xu H, Lu Q, et al. Madecassoside suppresses migration of fibroblasts from keloids: involvement of p38 kinase and PI3K signaling pathways. *Burns* 2012;38:677–684
45. Bernabei P, Bosticardo M, Losana G, et al. IGF-1 down-regulates IFN-gamma R2 chain surface expression and desensitizes IFN-gamma/STAT-1 signaling in human T lymphocytes. *Blood* 2003;102:2933–2939
46. Conti L, Regis G, Longo A, et al. In the absence of IGF-1 signaling, IFN-gamma suppresses human malignant T-cell growth. *Blood* 2007;109:2496–2504
47. Tu W, Cheung PT, Lau YL. Insulin-like growth factor 1 promotes cord blood T cell maturation and inhibits its spontaneous and phytohemagglutinin-induced apoptosis through different mechanisms. *J Immunol* 2000;165:1331–1336
48. Campbell CA, Burdick MD, Strieter RM. Systemic fibrocyte levels and keloid expression of the chemoattractant CXCL12 are upregulated compared with patients with normal scar. *Ann Plast Surg* 2021;87:150–155
49. Hong KM, Belperio JA, Keane MP, et al. Differentiation of human circulating fibrocytes as mediated by transforming growth factor-beta and peroxisome proliferator-activated receptor gamma. *J Biol Chem* 2007;282:22910–22920
50. Libura J, Drukala J, Majka M, et al. CXCR4-SDF-1 signaling is active in rhabdomyosarcoma cells and regulates locomotion, chemotaxis, and adhesion. *Blood* 2002;100:2597–2606
51. Hong KM, Burdick MD, Phillips RJ, et al. Characterization of human fibrocytes as circulating adipocyte progenitors and the formation of human adipose tissue in SCID mice. *FASEB J* 2005;19:2029–2031
52. Metz CN. Fibrocytes: a unique cell population implicated in wound healing. *Cell Mol Life Sci* 2003;60:1342–1350
53. Phillips RJ, Burdick MD, Hong K, et al. Circulating fibrocytes traffic to the lungs in response to CXCL12 and mediate fibrosis. *J Clin Invest* 2004;114:438–446

Pediatric Cavernomas - Dr Edward Smith MD MBA

Masterclass in Neurosurgery Lecture Series from the Neurosurgery research Listserv. Organized and Moderated by Dr G Narenthiran FEBNS FRCS. The Invited Lecturer is Dr Edward Smith MD MBA, Professor of Neurosurgery, Harvard College and Consultant Pediatric Neurosurgeon, Boston Children's Hospital. The lecture was delivered on Sunday 29 September 2024 at 12 GMT. Contact: g_narenthiran@hotmail.com
https://app.knowmia.com/7IRL

app.knowmia.com/ online recording available